Polymorphism of 17-β estradiol in a transdermal drug delivery system

N. E. VARIANKAVAL, K. I. JACOB*
School of Textile and Fiber Engineering, Polymer Education and Research Center, Georgia Institute of Technology, Atlanta, GA 30332-0295

S. M. DINH
Transdermals Pharmaceutical Research and Development, Novartis Pharmaceuticals, Suffern, NY 10901

The inclusions in a typical transdermal drug delivery system (TDS) containing estradiol drug were characterized using microscopic, spectroscopic and thermal analytical techniques. Optical and scanning electron microcscopy were used to determine the locations and morphologies of the crystals in the matrix. Two different types of crystals randomly distributed laterally inside the patch were observed. Solid aggregates were found surrounding needle-like inclusions. Optical imaging through the thickness of the patch and SEM sections of the patch revealed that these inclusions were found to occupy a single layer inside the adhesive matrix. No inclusions were observed either in the backing–matrix interface or the matrix–liner interface. The inclusions exhibited a wide range of sizes. The thickness of the crystals as determined by SEM ranged from 10–14 μm.

Out of the four crystal forms of estradiol, two of which are solvates (EA and EM) and the other two are anhydrous (EC and ED). Forms EC and ED did not exhibit significant differences in the spectra. Thermal analysis revealed that this was due to the highly unstable nature of ED and its tendency to either convert spontaneously to EC or occur in mixtures with it. The Raman spectrum of the aggregates in the patch showed peaks that seemed characteristic of at least two different forms of estradiol. Only one of these forms is a completely hydrogen bonded system and therefore, was concluded to be estradiol hemihydrate. A splitting of the C17–O peak at 1284 cm^{-1} and 1294 cm^{-1} was attributed to the existence of at least two types of crystal forms – one that exhibits hydrogen bonding and one that does not. DSC on different concentrations of estradiol in acrylic adhesive showed a clear endotherm for 14 wt % estradiol and apparent endotherms for lower concentrations. The absence of crystallization exotherms is due to the extremely slow kinetics of crystals growth in the polymeric patch.

Introduction

Transdermal drug delivery systems (TDS) are polymeric patches containing dissolved or dispersed drug that can deliver a drug at relatively constant rate to human body. Drug crystallization has been reported in many transdermal matrix systems [1–4] as well as other types of drug delivery systems [5–12]. Supersaturation of a drug in a TDS is often desirable in order to deliver a target therapeutic ''dose'' into the body since permeation rates of the drug through the patch and skin is dependent on the degree of saturation of the drug within a transdermal patch [4]. Polyacrylate adhesives generally have a high affinity for drugs which tends to solubilize higher concentrations of drugs than rubber adhesives like polyisobutylene [2]. However, acceptable permeation rates, and adhesive properties in particular, may not be achieved by systems consisting only of polyacrylate adhesives. In order to improve the adhesive properties of TDS (which could be essential in the long-term stability of the adhesive), a two polymer system, one in which the drug is soluble (e.g. polyacrylate) and another in which it is not (usually a rubber like polyisobutylene), has been employed. In this manner, the overall solubility of the drug in the adhesive system is reduced due to the incorporation of a component (in this case, the rubber) in which the drug is not soluble. This results in increased supersaturation thereby providing an environment conducive for crystallization of the drug.

The amount of drug that can be loaded in an adhesive is determined by its solubility in the adhesive. When this limit is exceeded, crystallization of the drug occurs due to supersaturation. The presence of crystals in a

*Author to whom all correspondence should be addressed.

transdermal patch might significantly affect the permeation of the drug through the patch, if dissolution of drug is the rate controlling step in the mass transfer process compared to the diffusion rate. Examples of decreased bioavailability were reported in the crystallization of nifedipine coprecipitated with polyvinylpyrrolidone (PVP) [9], indomethacin dispersed in a PVP matrix [10], and estradiol dispersed in polyacrylate adhesives stored over a period of six months at room temperature with moderate relative humidity [4, 5].

An investigation of phase changes in a drug provides a basis for understanding the dependence of drug permeation rate on microstructural interactions between a drug and an adhesive. Several studies have been reported on the physical interactions between adhesives and drugs [10, 13–14]. Almost all of these studies deal with the effect of adhesive microstructure and macroproperties (such as glass transition) on the diffusion coefficient of the drug in the adhesive. It is well known that the presence of a solute in a polymer reduces the T_g of the polymer and has been observed for the drug-in-adhesive system [15]. Using a modified WLF (Williams–Landel–Ferry) type equation, the effect of molar volume and chemical structure of the drug on its diffusion coefficient in the adhesive has been studied [16]. It was found that drugs with a secondary amido group interacted strongly with the acrylic adhesive, while those containing ester or acid groups did not. This is not surprising, since polar repulsions would prevent interactions of the latter type. An underlying assumption in all of the above studies is that the drug is present as a single phase inside the delivery system, which is not always valid. This assumption was probably valid in the above studies, because all measurements were made immediately after the patch had been formulated. It is possible that gradual phase transitions in the drug over a period of time would alter its physicochemical properties and also its delivery.

The only study in the literature that addresses the question of identifying the chemical structure of the crystals in transdermal systems was the Raman spectroscopic study on an estrogen patch, which was primarily concerned with mapping the distribution of drug inside the adhesive [17]. This mapping, however, was carried out on a certain area of a patch and no effort was taken to analyze the distribution of crystals along the thickness of the patch, which could be critical in terms of delivery kinetics. The researchers were able to identify a few crystals as that of a modified form of estradiol. Several techniques have been used to identify and characterize crystals in other forms of drug delivery systems. For example X-ray diffraction was used to quantify the presence of drug in an amorphous matrix [18]. NMR [19] and IR [20] spectroscopy have been used to characterize oral dosage forms and drugs dissolved in patches respectively, but the latter technique is not sensitive to crystallinity.

The presence of a modified crystal from inside the patch could affect the physicochemical nature of the drug, its diffusion through the patch and thereby, its bioavailability. This investigation would be the first step in identifying conditions under which crystal-free patches could be produced. Different crystal forms found in a typical TDS with estradiol (Fig. 1) drug are characterized in this study.

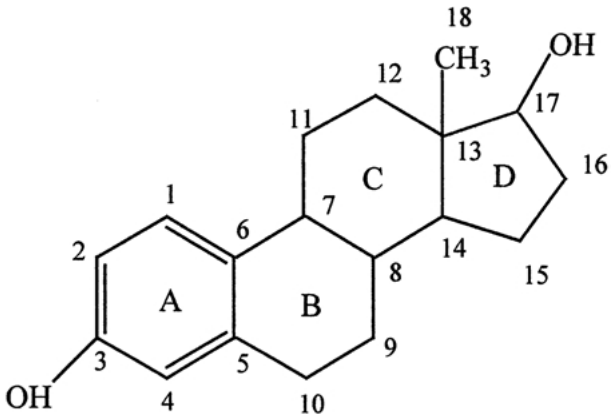

Figure 1 Schematic representation of the estradiol molecule. The numbers represent the naming system of the carbon atoms in the molecule and alphabets represent the four ring systems in estradiol.

Materials and methods

Materials

Estradiol hemihydrate (EA), obtained from Sigma, and transdermal patches obtained from Novartis Pharmaceuticals Corporation, were used as received. The estradiol crystals in the patch will be denoted by CP. Pressure sensitive acrylic adhesives were obtained from National Starch and Chemical Company (DURO-TAK 87-2852). The adhesives are supplied in solution form in a mixture of four solvents – ethyl acetate, toluene, isopropanol and *n*-hexane. This adhesive was coated onto a release liner (ScotchPak, 3M Pharmaceuticals) and oven-dried at a temperature of 65 °C for about 2 h to a final thickness of about 25 mil (0.635 mm). Thermogravimetric analysis of a portion of the coated adhesive did not reveal the presence of any of the solvents listed above.

Preparation of EC and ED

Two anhydrous forms of estradiol, represented as EC (Form C) and ED (Form D), were used in this study. EC was prepared by melting EA and subsequent slow cooling of the melt. ED was prepared by melting EA and rapidly quenching the melt with liquid nitrogen. An alternate method of preparation was by crystallizing it from a boiling ethyl acetate solution on a hot plate. This produced ED that had exhibited identical properties with that prepared by the first method.

Estradiol in acrylic adhesive films

Four different concentrations of estradiol in acrylic adhesive were prepared by blending the desired weight of estradiol hemihydrate in an adhesive solution and stirring until complete dissolution was achieved. The solution was then cast in petri dishes and dried in a vacuum oven at 40 °C for three days to completely remove the solvent. These films were then used for thermal analysis.

TABLE I Raman spectral comparison of crystal forms of estradiol and the aggregate crystals in the transdermal patch

A	C	D	CP	Assignment
Polar groups				
1283	1281	1283	1285	δ(O17-H)
1254	1252	1254	1255	CH3 rock
1237	1233, 1240	1239		ν(C3-O)
Non-polar groups				
252	248, 258	248, 255		$\tau(CH_3)$
				δ (CCC)
363, 373	363, 375, 386		374	δ (CCC)
724	724	722	722	δ (CCC)
733	733	732	732	aromatic ring breathing
830	829	830	830	δ_s(C1, C2-H)
928	930	928	928	δ_{as}(C1-C2-H)
1006	1005	1006	1006	ν(C-C-H)A
	1215			CH_2D
1254	1252	1254	1240	CH_3rock
				δ_s(C18-H)
1451	1450	1452	1455	ν(C-C-H)B, C, D
				ν(C-C-H) A
1586	1585	1586		$\nu(C\text{-}C)_{as}$ whole ring

Methods

Optical microscopy

Optical microscopy was carried out using a Leitz Laborlux 12 POL polarized optical microscope with a maximum magnification of 400 ×. The samples (transdermal patches) were mounted on glass slides. A drop of ethylene glycol was placed on the patch to eliminate the effects of optical interference by the air/sample interface. A glass coverslip was then placed on the sample and images were taken with a camera attached to the microscope. The polarizer and analyzer were adjusted to crossed positions to obtain greatest polarization, when viewing samples that contained crystals. This position was found to yield the greatest contrast between the crystals and the matrix. Micrographs of the adhesive matrix, backing membrane, and release liner were taken with the polarizers in place, but not crossed. Clearer micrographs were obtained by this method. The aperture size was also carefully adjusted to maintain the clarity of the micrographs. The microscope was equipped with a camera so that live pictures could be taken. The camera was interfaced with an image analysis software, Video Matrox Meteor, which was used to record the images.

Scanning electron microscopy

SEM studies were carried out on a Hitachi 800 instrument operating at an accelerating voltage of 10 kV. The extraction voltage was 3.8 kV and the operating current was 10 μA. All micrographs were obtained at a magnification of 350 × at three different locations inside the patch. Four samples were analyzed.

Raman microspectroscopy

This technique was used to characterize the chemical and physical natures of the solid inclusions in the transdermal systems. The advantage of Raman microspectroscopy arises from the fact that incident light can be focused on a relatively small area (e.g. a circle of radius 2 μm) to obtain a Raman spectrum. The microscope can be focused to different depths in the sample. Raman spectroscopy was per-formed on a Kaiser Holoprobe Raman Microspectro-meter with a solid diode laser operating at 758 nm, with backscattering optics. All the spectra were obtained with 5 accumulations, each of 30 s. duration. The region of focus on the sample was a circle, 2 μm in diameter. The plane of focus was that in which the crystals were present. The depth was approximately 200–250 μm from the upper surface of the backing. Optical micrographs (bright field images) were taken at a magnification of 16 ×. Spectral assignments used in this study are listed in Table I.

Differential scanning calorimetry

Differential scanning calorimetry was carried out in a SETARAM thermal analysis system. All runs were carried out from 25 to 210 °C. The upper limit was determined by the expected melting point of estradiol hemihydrate which is in the range 176–182 °C. Nitrogen was used as the purge gas in ambient mode. The heating rate was kept at a constant 10 °C min^{-1}.

Hot stage microscopy

A heating stage was attached to the Leitz Laborlux 12 POL instrument used in optical microscopy studies. The temperature was monitored by a thermocouple lead, which was attached to the heating stage. No specific heating rate was required and hence a controller was not used. The samples were mounted on cover glass slips and placed in the insulated compartment on the stage. Micrographs were taken at the temperatures at which melting (or dissolution) was observed.

Results and discussion

Morphology and distribution of crystals in the matrix

Optical micrography was used to determine the location and sizes of the solid inclusions formed inside the

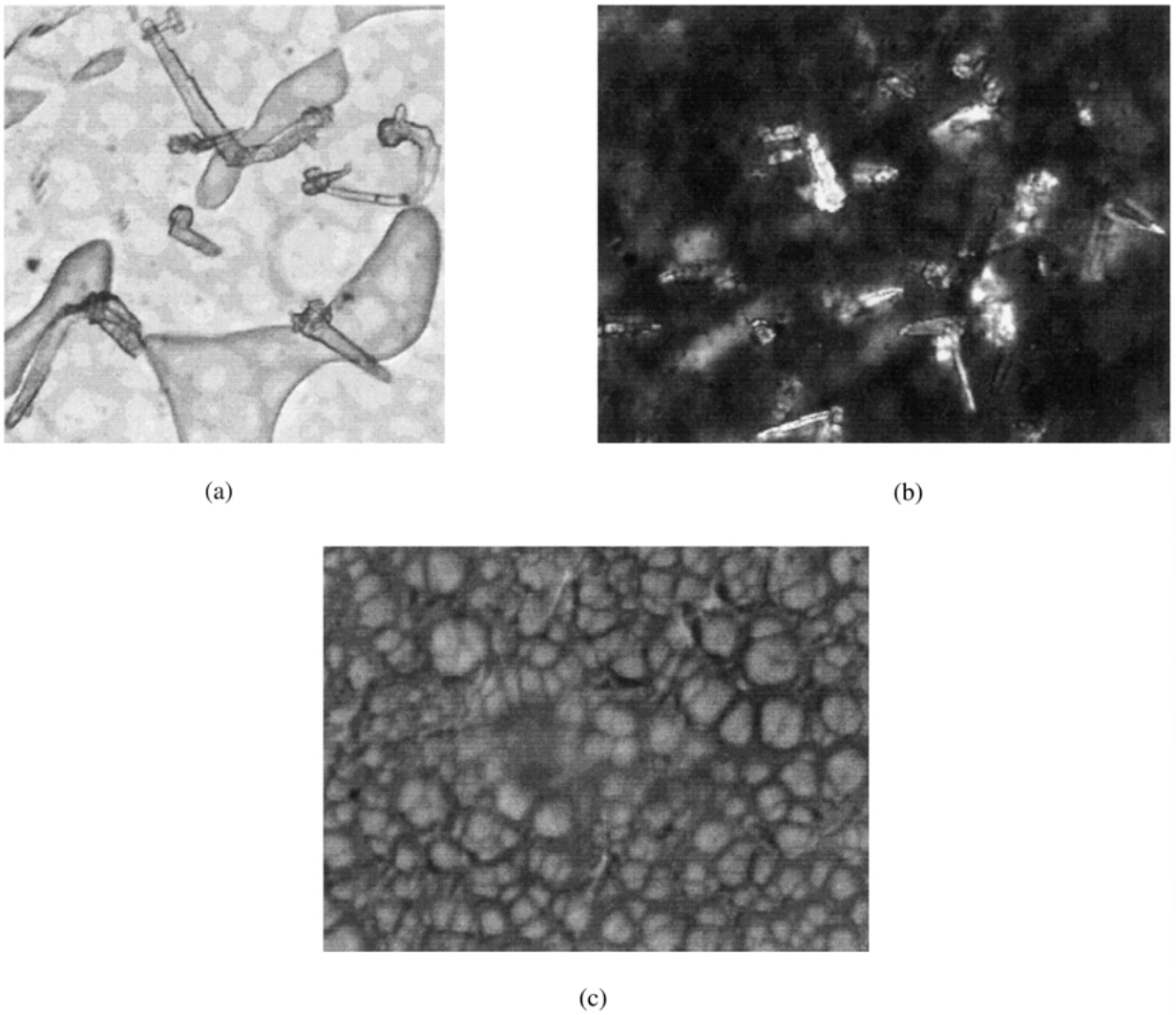

Figure 2 Optical micrographs of crystals in the patch observed under (a) non-polarized and (b) polarized conditions. This patch had been in storage for about a year. (c) Optical micrograph of a freshly formulated transdermal patch with no crystals. The magnification used in all three cases was 16 × .

adhesive patch which are six months or older. These two factors could have significant influence on the distribution of the drug in the matrix and its subsequent diffusion through the adhesive. The morphology of the solid precipitates[1] in the matrix (adhesive) can be seen in Fig. 2. The solids were dispersed throughout the patch. The majority of these solid dispersions were needle-like. Aggregates of other particles could also be seen around these needles. When viewed under crossed polarizers, these dispersions appeared much brighter compared to the surrounding matrix, with a definite structure associated with them. This enabled their identification as crystals. The presence of crystals in the patch assumes significance considering the fact that these were not present when the patches were formulated. An optical micrograph of a typical newly formulated patch is shown in Fig. 2(c).

By adjusting the focus of the microscope, it was possible to obtain micrographs of different layers within the patch. The vertical dimensions of the patch could be measured approximately by calibrating the distance moved by the microscope stage vertically. The backing membrane was approximately 50 μm thick. The microstructure of the patch at different layers can be seen clearly in Fig. 3. It was observed that the crystals occupied a single layer near the center of the patch. There were no crystals either near the backing-adhesive interface or the adhesive-liner interface. This shows that these interfaces have no effect on the crystallization observed in this system. The thickness of the adhesive matrix layer was approximately 50 microns. The variation in thickness between different patches was not significant.

The sizes of the needle-like crystals were approximately 4–6 μm × 9–11 μm. There was considerable variation in the size range of the crystals. Due to this reason, it was not possible to measure the size of the clusters around the needles.

Scanning electron microscopy was employed to determine the dimensions of crystals in the patch-particularly across the thickness. Thin strips of the patch were made, by cutting at different locations. The patches were then mounted vertically in order to view across their thickness. SEM images of the cross-section were then obtained. Using this technique however no distinction between the two different types of crystals could be made. The SEM scans also showed that the crystals were mainly found in the central region of the

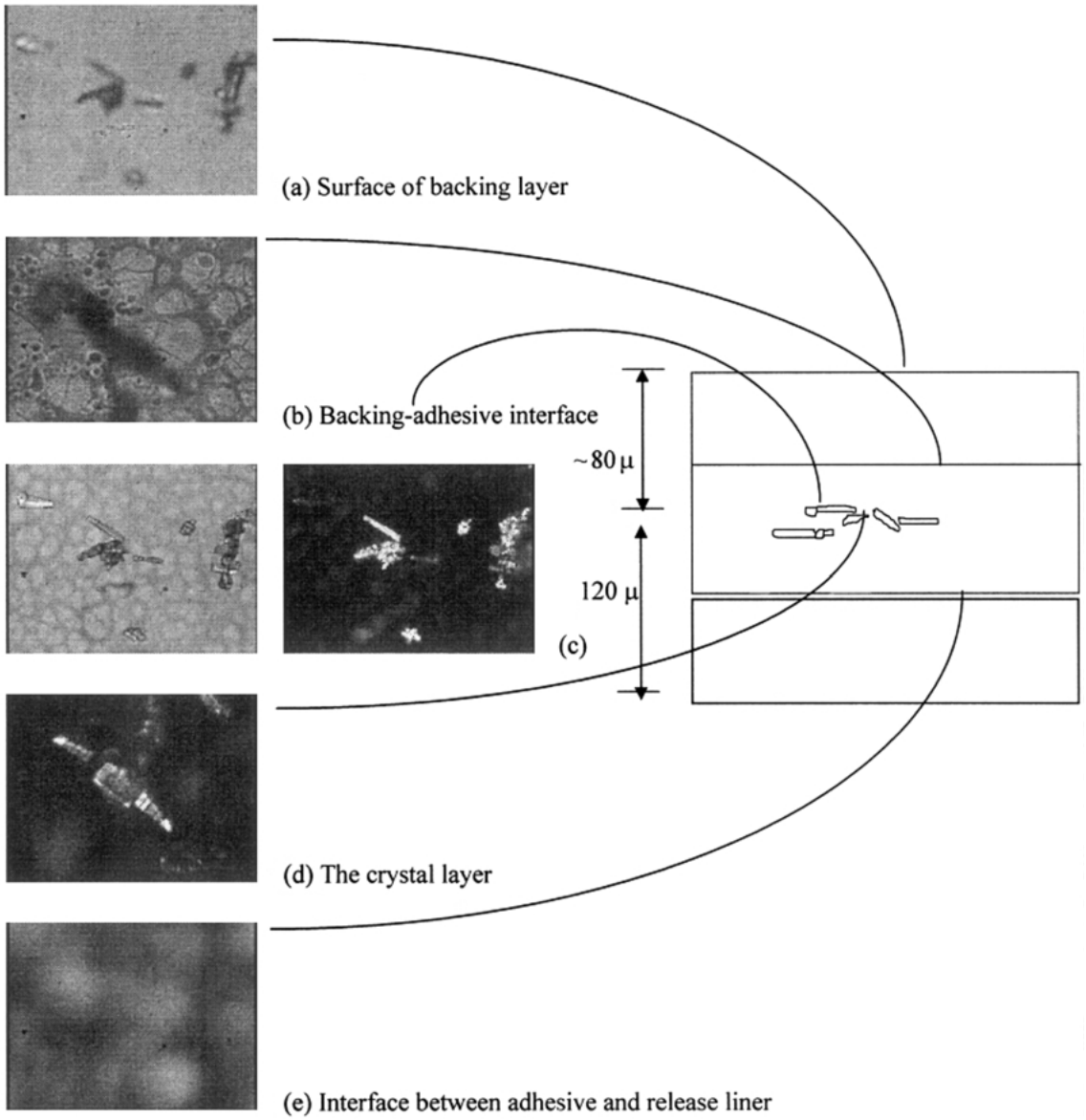

Figure 3 Optical micrographic scan through the thickness of the patch. The polarizer and analyzer were crossed in figures (c) and (d) to obtain better contrast and to identify the crystals. A magnification of 16 × was used for micrographs (a), (c) and (e). A higher magnification (40 ×) was used for (b) and (d) to study the morphology. The two figures in (c) are of different brightness because the intensity of the lamp was adjusted to obtain better contrast.

patch. The interfaces were free of crystals. The thickness of the crystals ranges from 10–14 μm as can be seen from the sample SEM micrographs in Fig. 4.

Thermomicroscopy

This method provides a means of observing the melting of crystals. Fig. 5 shows the optical micrographs of the patch as a function of temperature. The crystals in the patch at room temperature are clearly seen in Fig. 5(a). On heating the patch, the aggregated crystals around the patch first melted around 134–136 °C followed by the complete melting of the needles around 146 °C. This difference in the melting ranges for these two types of crystals indicated that their physical and/or chemical constitution were different. The much lower melting point of the estradiol crystal aggregates was due to the increase in solubility of estradiol in the adhesive with increasing temperature. Thus, the crystals dissolved in the surrounding matrix at a much lower temperature than they normally would in their pure crystalline state.

Thermal analysis

DSC studies were carried out on four different concentrations of estradiol hemihydrate dissolved in acrylic adhesive and are shown in Fig. 6 with the accompanying Table II. The heating curves for three samples barely showed melting endotherms. An analysis of magnitude of the heats of melting, casts some doubt about the nature of these apparent endotherms. No conclusion is therefore made based on these results. No exothermic transitions were observed in the cooling curves. The film with highest concentration of estradiol (14 wt %) showed a melting endotherm around 140 °C. This was identical to the melting endotherm observed in thermomicroscopy of the transdermal patches. The absence of clear exotherms for lower concentrations is

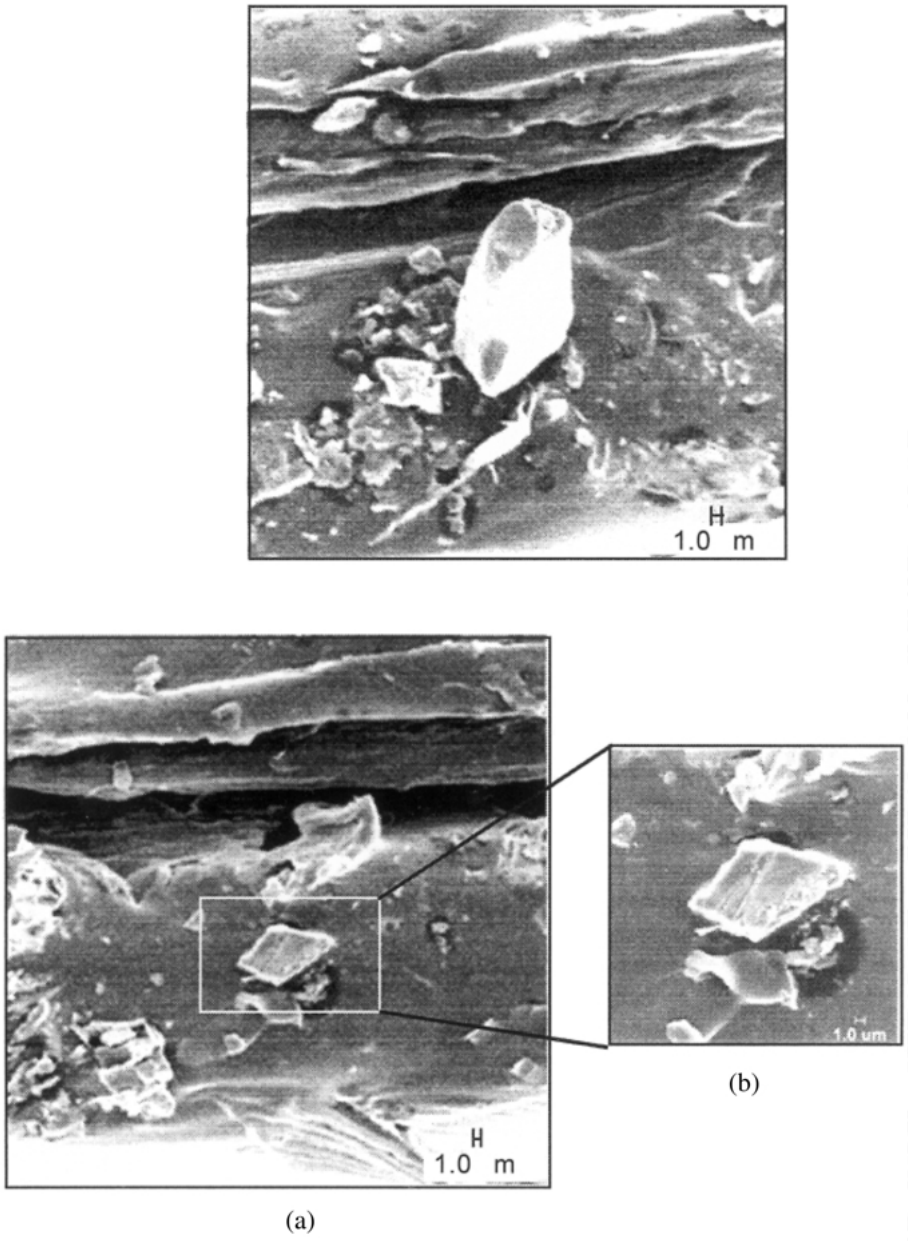

Figure 4 Scanning electron micrographs of the cross section of transdermal patches containing crystals of estradiol. Two representative samples are shown in the figure. All micrographs were obtained at an accelerating voltage of 10 kV; (b) is a magnification of the area shown in (a).

apparent when one considers the fact that crystallization in patches occurs over a time scale of months.

The molecular conformation of estradiol is intimately related to its biological activity [21]. The conformation is in turn dictated by the specific crystal structure adopted by estradiol. It is evident from Raman studies that estradiol does not completely crystallize as estradiol hemihydrate inside the transdermal patch. Depending upon the crystallization conditions, estradiol may form one of several modifications.

Raman microspectroscopic investigations

This study is organized as follows. First, the entire spectrum is divided into four regions characteristic of steroids in terms of vibrational modes [22], and the spectrum of estradiol is then interpreted on this basis. Next, an analysis of the solid state of the inclusions is carried out. Finally, the chemical nature of the crystals is deciphered.

Spectral region 4000–2800 cm^{-1}

The vibrations of a C–H bond on a double bonded or aromatic carbon atom – 3030–3070 cm^{-1} is very strong in the Raman spectrum compared to the IR spectrum.

Spectral region 2800–1350 cm^{-1}

The stretching vibrations of the isolated C = C bonds – 1620–1672 cm^{-1} are very strong in the Raman spectrum. These vibrations would show almost zero intensity in the infrared spectrum. Aromatic rings show two bands of medium intensity in the IR and Raman spectra near 1600 cm^{-1}. This is clearly evident in Fig. 7. Steroids with aromatic rings show their strongest bands below 1450 cm^{-1}, as can be seen in the case of estradiol hemihydrate. Near 1450 cm^{-1}, the bending of CH_2 groups and the degenerate bending of CH_3 groups show bands of medium intensity in the Raman spectra. These

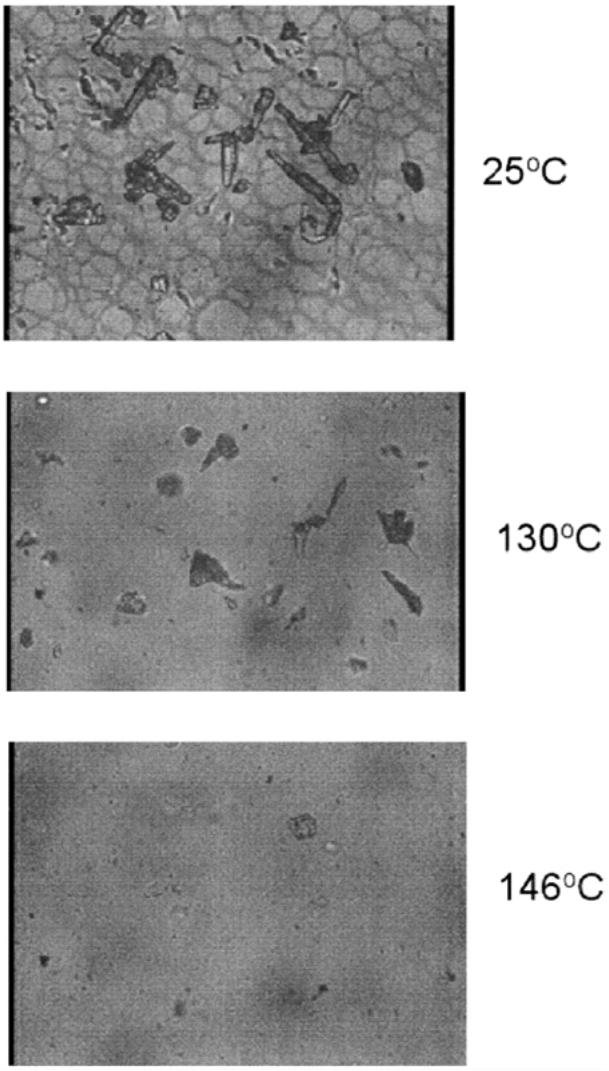

Figure 5 Thermomicroscopy of transdermal patches as received. The patches had been in storage for about a year. A scanning rate of 10 K min^{-1} was used.

are often used as internal standards for identifying the steroid skeleton [22].

Spectral region 1350–800 cm^{-1}

This region consists of the wagging, twisting and rocking deformations of the C–H bond and the stretching vibrations of the skeleton. The most important vibration for this study in this region is the CH_3 rock, found near 1250 cm^{-1} [22].

Spectral region 800–200 cm^{-1}

Presence of an aromatic ring is substantiated by a strong band near 725 cm^{-1}. This can be seen in the spectra of

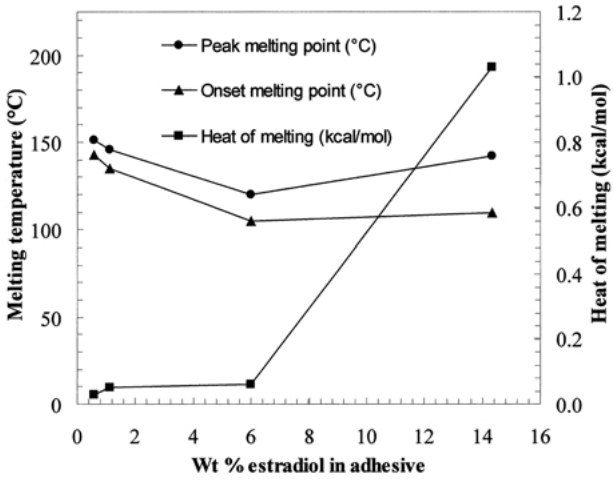

Figure 6 Variation of the melting temperature and heat of melting of estradiol in acrylic adhesive as a function of estradiol concentration in adhesive.

estradiol hemihydrate and the crystals grown from methanol.

Spectral region 200–20 cm^{-1}

Crystalline steroids show bands of medium to strong intensity in this region of the Raman spectrum that can be assigned to translational and torsional (librational) vibrations of rigid molecules. The intensity of these vibrations is especially high when a molecule has appreciably different electron polarizability along its main axis of inertia. The focus for estradiol would be the bands found in the 70–110 cm^{-1}

Raman microscopic studies

It was apparent from an earlier investigation that there might be more than one form of crystal in the transdermal patches, since estradiol crystals are known to exits in four different forms. The analysis presented in this paper restricts itself to the study of crystalline aggregates of 17-β estradiol in the patch. Samples of crystal forms EA, EC, ED and CP were chosen for spectral analysis comparison. Form EM was excluded since it was proven to be a solvate crystal and not a true polymorph. Spectral comparisons were carried out between the various polymorphic forms of estradiol and crystals of estradiol in the patch and the assignments are listed in Table I. This also provided an opportunity to study the chemical characteristics of the three crystal forms.

The entire Raman spectrum of estradiol is divided into four regions. The region from 0–500 cm^{-1} is very

TABLE II Variation of melting point, heat of melting and degree of crystallinity with concentration of estradiol in the adhesive

Con. of estradiol estradiol wt (%)	Peak m.pt. °C	Onset m.pt. °C	Heat of melting kcal/mol	Degree of crystallinity*
14.32	142	110	1.03	0.105
6.00	120	105	0.06	0.006
1.11	146	135	0.05	0.005
0.58	151	143	0.03	0.003

* The degree of crystallinity was based on the heat of melting of pure estradiol hemihydrate (9.8 kcal mol^{-1}).

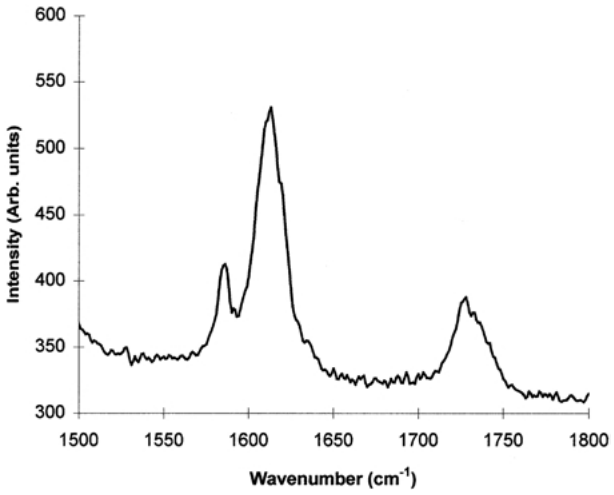

Figure 7 Two bands of medium intensity near 1600 cm^{-1} prove the presence of the aromatic ring system. The intensity along the *y*-axis is provided only for visualization.

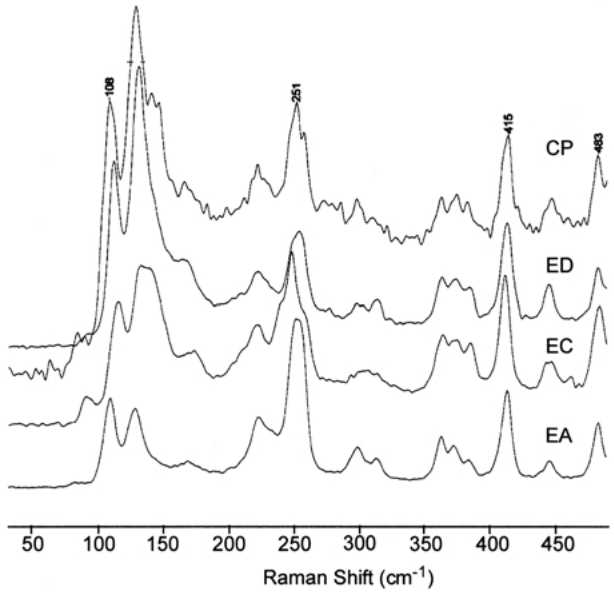

Figure 8 Raman spectral comparison between the crystal forms of estradiol and the aggregates in the patch. The low wavenumber region is sensitive to crystal structure. The vertical axis represents intensity in arbitrary units.

sensitive to crystal structure and is shown in Fig. 8. The bulk of the chemical structure details can be obtained from the region 500 cm^{-1} to about 2000 cm^{-1} and is shown in Figs 9 and 10. The spectra of EC and ED were similar in most respects. This is because of the tendency of Forms EC and ED to occur in mixtures, giving rise to a mixed Raman spectrum for EC and ED, and two distinct melting endotherms in DSC studies. There were only minor differences in the low wavenumber region. This observation is in agreement with the results from thermal analysis. The first heating segment were identical for both forms while the second heating segment revealed two endotherms, corresponding to the simultaneous presence of two different forms. The resonances at 108 and 129 cm^{-1} were almost of equal intensity in EA while they were appreciably different in EC and ED (cf. Fig. 8), which is attributed to the differences in the nature of the crystal packing. The resonances exhibited by CP in this region, for the most part coincided with those shown by

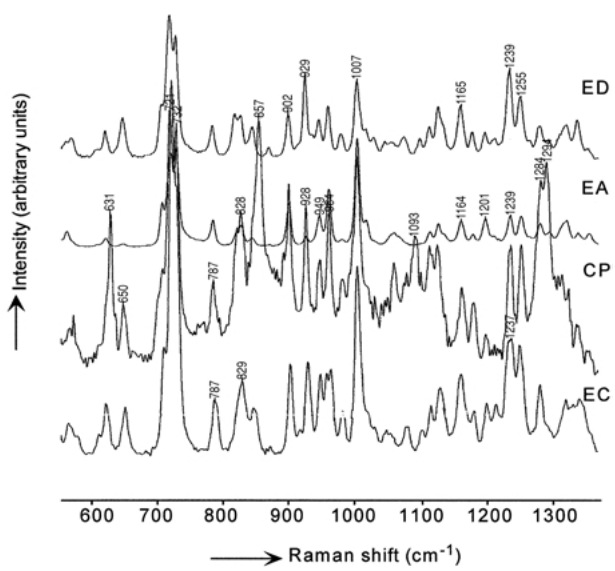

Figure 9 Raman spectral comparison between the crystal forms of estradiol and the aggregates (CP) in the patch.

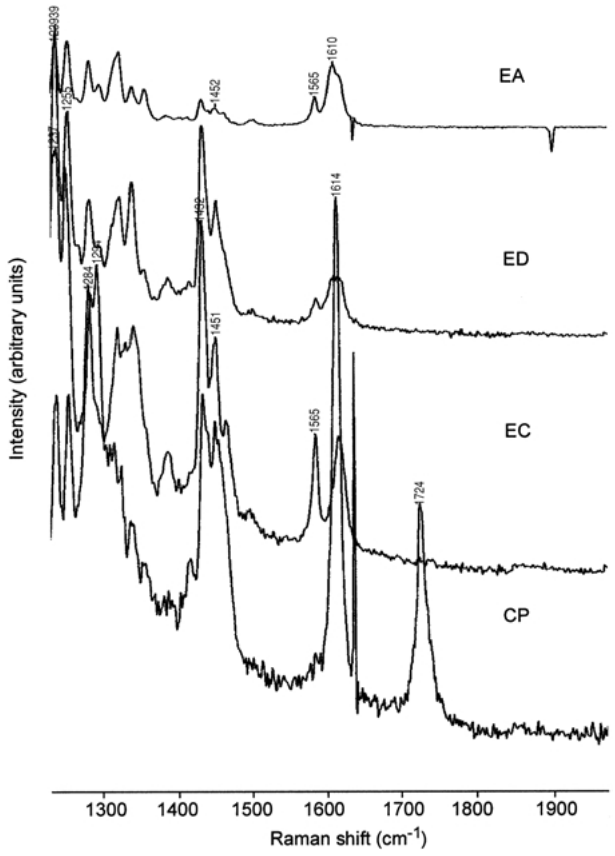

Figure 10 Raman spectral comparison of the 1300–1700 cm^{-1} region for the crystal forms and the aggregate in the patch.

EC and ED. The shoulder of the peak at 251 cm^{-1}, which is associated with the $\tau(CH_3)$ stretch, was observed in EC and CP. This was conspicuously absent in the other two spectra. The reason for its absence in the other two forms was not apparent.

The bands at 631 and 650 cm^{-1} were strong in the spectra of EC, ED and CP, but less pronounced in EA. These bands are associated with aromatic stretching which should be a common feature of all samples. The strong peak at ca. 855 cm^{-1} in the spectra of CP probably arises from the matrix and could be seen as a

strong resonance in the spectrum of the adhesive, but not in the other samples. The aromatic stretch around 1006 cm^{-1} was very strong in all four samples.

The δ(OH) bands of secondary and tertiary alcohols absorb in the 1200–1350 cm^{-1} range. This vibration mode is sensitive to hydrogen bonding. The spectra of EA, EC and ED all exhibit a single peak at 1282 cm^{-1}, attributed to δ(O17-H). In the spectrum of CP, this band was split into a doublet (1284 cm^{-1} and 1294 cm^{-1}) implying that the O17-H moiety, which gave rise to this peak, was present in two different environments in terms of hydrogen bonding. The low frequency stretch (1284 cm^{-1}) corresponded to the free δ(O17-H) vibrations, while that at 1294 cm^{-1} was characteristic of a bonded O–H vibration. A similar behavior was observed in the spectrum of ethynylestradiol for which it has been established that two types of hydrogen bonding exist [23]. The presence of a peak splitting corresponding to ν(C17-O) near 1046–1056 cm^{-1} would confirm this dual hydrogen-bonding behavior. The Raman spectrum of CP is less resolved in this region than that corresponding to either EA, EC or ED, the first of which exhibits a single type of hydrogen bonding while the other two are anhydrous forms, and hence incapable of intermolecular hydrogen bonding through water. As ν(O17-H) is sensitive to structural changes in the estradiol molecule, the pressure dependence of the O–H stretching vibration has been studied in order to determine the sensitivity of ν(O17-H) to structural changes. At high pressures, the ν(O17-H) band is split into two because of different pressure behavior exhibited by the two forms of hydrogen bonding. The high-energy peak corresponded to the non-hydrogen-bonded form. Upon hydrogen bonding, the vibrational energies of bands associated with hydrogen bonding are reduced due to loss of electron density into the hydrogen bond. This particular band is, of course, not prominent in the Raman spectrum, as the technique is not sensitive to vibrations of polar groups.

Conclusions

The inclusions in an estradiol TDS patch were characterized using microscopic, spectroscopic and thermal analytical techniques. Optical microscopy was used to determine the locations and morphologies of the estradiol crystals in the matrix. Two different types of crystals are observed inside the patch, distributed randomly in the lateral direction. Solid aggregates were found surrounding needle-like inclusions. Optical imaging through the thickness of the patch revealed that these inclusions were found to occupy a single layer inside the adhesive matrix, which was further confirmed by SEM images. No inclusions were observed either in the backing–matrix interface or the matrix–liner interface. The inclusions exhibited a wide range of sizes. The thickness of the crystals, as determined by SEM, ranged from 10–14 μm.

The Raman spectrum of the aggregates in the patch showed peaks that seemed characteristic of at least two different forms of estradiol. Only one of these forms is a completely hydrogen bonded system and therefore, was concluded to be estradiol hemihydrate (EA). A splitting of the C17-O peak at 1284 and 1294 cm^{-1} was attributed

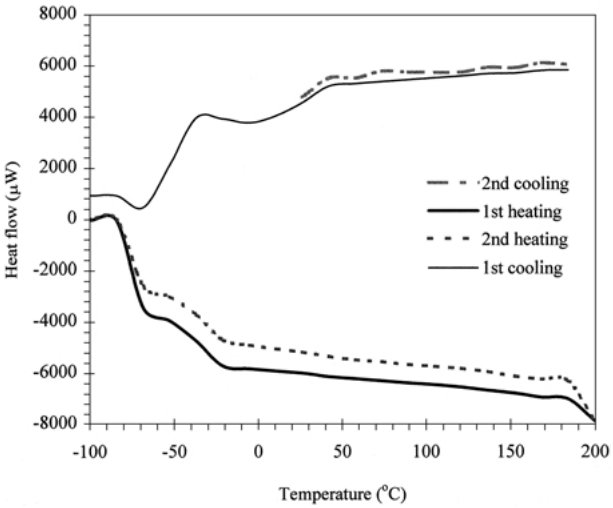

Figure 11 DSC scans of the placebo patch. The glass transition of the adhesive is seen at ca. −40 °C. No other thermal transitions occur in the patch. All heating and cooling rates were maintained at 5 °C min^{-1}.

to the existence of at least two types of crystal forms – one that exhibits hydrogen bonding and one that does not. Thus, it is evident that estradiol crystals exists in the hemihydrate form in the TDS patches. The other form of estradiol crystals in the patch, which does not exhibit hydrogen bonding, could only be identified as EC or a mixture of EC and ED. Exact identification of the crystal form was difficult with the methods used in this investigation because EC and ED did not exhibit significant differences in the Raman spectra, and due to the highly unstable nature of ED and its tendency to either convert spontaneously to EC or occur in mixtures with it as shown by thermal analysis.

Since these patches do not contain any crystals immediately after they were produced, the kinetics of crystallization is controled, to a large extend, by the availability of water molecules to form estradiol crystals in their most stable estradiol hemihydrate form. Further work is needed to determine the source of water molecules that enabled this crystallization. Also, the presence of anhydrous crystal forms of estradiol in the patch shows that even in the absence of water, crystallization is possible for estradiol in the TDS patch.

Thermal analysis of placebo acrylic patches did not show any evidence of crystallization (cf. Fig. 11). DSC carried out on acrylic patches with different concentrations of estradiol showed a clear endotherm for 14 wt % estradiol and less pronounced endotherms for lower concentrations indicating possible nucleation and crystallization of estradiol. For drug concentrations approaching that of the TDS, the endotherms were ambiguous and crystallization of estradiol could not be concluded form the data. The absence of clear crystallization exotherms is due to the extremely slow kinetics of crystals growth in the polymeric patch.

Notes

1. The words precipitates and inclusions are used interchangeably throughout the discussion. Precipitate implies that some component of the transdermal system passes from the solid–solution phase to a solid phase. An inclusion simply refers to a solid state dispersion of one material in another.

Acknowledgment

The authors are grateful to Novartis Pharmaceuticals for financial support.

References

1. J. MIRANDA and S. SABLOTSKY, US Patent #WO 95/18603, Noven Pharmaceuticals (1995).
2. J. MIRANDA and S. SABLOTSKY, US Patent, PCT US95/00022, Noven Pharmaceuticals (1995).
3. M. XINGHANG, J. TAW and C. CHIANG, *Proc. Int'l Symp. Control. Rel. Bioact. Mater.* **22** (1995) 712.
4. M. XINGHANG, J. TAW and C. CHIANG, *Int. J. Pharm.* **142** (1996) 115.
5. A. P. SIMONELLI, S. C. MEHTA and W. I. HIGUCHI, *J. Pharm. Sci.* **59**(5) (1970) 633.
6. K. H. ZILLER and H. H. RUPPRECHT, *Pharm. Ind.* **52**(8) (1990) 1017.
7. I. SUGIMOTO, A. KUCHIKI and H. NAKAGAWA, *Chem. Pharm. Bull.* **29** (1981) 6.
8. M. YOSHIOKA, B. C. HANCOCK and G. ZOGRAFI, *J. Pharm. Sci.* **84**(8) (1995) 983.
9. K. UEKAMA, K. IKEGAMI, Z. WANG, Y. HORIUCHI and F. HIRAYAMA, *J. Pharm. Pharmacol.* **44** (1992) 73.
10. R. TODDYWALA, K. ULMAN, P. WALTERS and Y. W. CHIEN, *Int. J. Pharm.* **76** (1991) 77.
11. F. STEFANO and F. BIOALI, *Proceed. Int'l Symp. Control. Rel. Bioact. Mater.* **24** (1997) 703.
12. T. CARRIG and D. THERRIAULT, *ibid.* **24** (1997) 891.
13. T. KOKUBO, K. SUGIBAYASHI and Y. MORIMOTO, *Pharm. Res.* **11**(1) (1994) 104.
14. R. LICHTENBERGER and H. P. MERKLE, *Int. J. Pharm.* **64** (1990) 117.
15. F. BUECHE, ''The Physical Properties of Polymers'' (Wiley & Sons, New York, 1962).
16. Y. MORIMOTO, T. KOKUBO and K. SUGIBAYASHI, *J. Controlled Release* **18** (1992) 113.
17. C. L. ARMSTRONG, H. G. M. EDWARDS, D. W. FARWELL and A. C. WILLIAMS, *Vib. Spec.* **11** (1996) 105.
18. S. R. BYRN, ''Solid-State Chemistry of Drugs'' (Academic Press, New York, 1982).
19. A. SALEKI-GERHARDT and G. ZOGRAFI, *Pharm. Res.* **11** (1994) 116.
20. C. A. OKSANEN and G. ZOGRAFI, *ibid.* **10**(6) (1993) 791.
21. E. G. SALOLE, *J. Pharm. Biomed. Anal.* **5**(7) (1987) 635.
22. E. HEFTMANN, ''Modern Methods of Steroid Analysis'' (Academic Press, New York, 1973).
23. T. ISHIDA, M. DOI, M. SHIMAMOTO, N. MINAMINO, K. NONAKA and M. INOUE, *J. Pharm. Sci.* **78** (1989) 4.

Received 8 September 1999
and accepted 29 June 2001